1 All driven by energy demand? Integrative comparison of metabolism of *Enterococcus faecalis*

2 wildtype and a glutamine synthase mutant

3

4 Seyed Babak Loghmani[1], Eric Zitzow[2], Gene Ching-Chiek Koh[3#], Andreas Ulmer[4], Nadine Veith[1],

5 Ruth Großeholz[1], Madlen Rossnagel[2], Maren Loesch[4], Ruedi Aebersold[3], Bernd Kreikemeyer[2],

6 Tomas Fiedler[2], Ursula Kummer[1]

7

8 [1]Department of Modelling of Biological Processes, BioQuant/COS Heidelberg, Heidelberg

9 University, 69120 Heidelberg, Germany

10 [2]Institute for Medical Microbiology, Virology and Hygiene, Rostock University Medical Centre,

11 Schillingallee 70, 18057 Rostock, Germany

12 [3]Department of Biology, Institute of Molecular Systems Biology, ETH Zurich, Zurich Switzerland

13 [4]Institute of Biochemical Engineering, University of Stuttgart, Stuttgart, Germany

14 [#]Current address: MRC Cancer Unit, University of Cambridge, Cambridge CB2 0XZ, UK

15

16 Abstract

17 Lactic acid bacteria (LAB) play a significant role in biotechnology, e.g. food industry, but also

18 in human health. Many LAB genera have developed a multidrug resistance in the past few

19 years, becoming a serious problem in controlling hospital germs all around the world.

20 *Enterococcus faecalis* accounts for a large part of the human infections caused by LABs.

21 Therefore, studying its adaptive metabolism under various environmental conditions is

22 particularly important. In this study, we investigated the effect of glutamine auxotrophy

23 (Δ*glnA* mutant) on metabolic and proteomic adaptations of *E. faecalis* in response to a

24 changing pH in its environment. Changing pH values are part of its natural environment in the

25 human body, but also play a role in food industry. We compared the results to those of the

26 wildtype. Our integrative method, using a genome-scale metabolic model, constrained by

27 metabolic and proteomic data allows us to understand the bigger picture of adaptation

28 strategies in this bacterium. The study showed that energy demand is the decisive factor in

29 adapting to a new environmental pH. The energy demand of the mutant was higher at all

30 conditions. It has been reported that Δ*glnA* mutants of bacteria are energetically less effective.

31 With the aid of our data and model we are able to explain this phenomenon as a consequence

32 of a failure to regulate glutamine uptake and the costs for the import of glutamine and the

33 export of ammonium. Methodologically, it became apparent that taking into account the non-

34   specificity of amino acid transporters is important for reproducing metabolic changes with

35   genome-scale models since it affects energy balance.

36

37   Introduction

38

39   Lactic acid bacteria (LAB) are gram-positive microorganisms, fermenting hexose sugars to

40   lactic acid as their primary product under many conditions. Among LABs there are both

41   pathogenic as well as commensal species. In some cases, e.g. in the case of *Enterococcus*

42   *faecalis* (*E. faecalis*) both commensal, as well as pathogenic behavior occurs[1]. As a part of the

43   commensal flora, *E. faecalis* colonizes different tracts in the human body, especially the gut.

44   Due to its pathogenic potential, *E. faecalis* frequently causes nosocomial infections, most

45   commonly of the urinary tract, but also soft tissue or intra-abdominal infections, bacteremia

46   or endocarditis[2]. An increasing proportion of *E. faecalis* strains isolated from such infection

47   shows multidrug resistance against a wide range of antibiotics[3,4]. The treatment of infections

48   caused by these multi-resistant *E. faecalis* strains can be remarkably hard and may cause

49   severe problems in hospital environments[5].

50   On the other hand, *E. faecalis* strains generally regarded as safe (GRAS) are used in food

51   industry as a cheese starter culture[6] or as a probiotic[7]. The intended probiotic isolates,

52   however, should undergo screening to ensure the absence of transferable virulence factors

53   and antibiotic resistant genes[8]. Hence, *E. faecalis* encounters very different native

54   environments ranging from different human body tissues to different kinds of food. This

55   requires enormous flexibility of the metabolism of *E. faecalis* that in turn would be reflected

56   by various metabolic phenotypes.

57

58   To gain a comprehensive understanding of metabolic phenotypes, the cell-wide and

59   integrative analysis of metabolism is central. This is something that pure experimental

60   research cannot deliver, and therefore, different computational approaches have been

61   developed to study metabolic networks. For smaller networks and more detailed analysis,

62   kinetic models based on ordinary differential equations (ODEs) are the best choice[9]. When

63   integrating all reactions of the metabolic network and in the absence of detailed kinetic data,

64   genome-scale metabolic models, as used below, are nowadays the preferred and most

65   commonly used strategy. Genome-scale metabolic models are stoichiometric representations

66 of all annotated metabolic reactions in a given cell which allow the computation of flux

67 distributions based on the knowledge of their localization, wiring and the biomass

68 composition of the specific organism and/or cell type[10]. Optimal flux distributions are

69 calculated according to an optimality criterion like biomass maximization[11]. This is an

70 especially successful criterion for investigating microorganisms since these often follow

71 relatively simple principles like optimizing growth. However, the typical outcome of such an

72 optimization (flux balance analysis (FBA)) is not a unique solution and the huge size of the

73 solution space renders interpretation of the results difficult and error-prone[12]. By adding

74 constraints, e.g. through experimentally measured medium composition, input and output

75 fluxes of metabolites[13], transcriptome[14], as well as proteome data[15] the solution space can

76 effectively be decreased and the predictive power of the models increased[15,16].

77

78 In this study, we analyzed the metabolic and proteomic profile of a knock-out mutant of

79 glutamine synthetase (Δ*glnA)* of the multiresistant *E. faecalis* V583 strain during a pH shift

80 experiment. Glutamine Synthetase (GlnA) is a vital protein as it is the main enzyme in the

81 assimilation of ammonia and has an overall control over the nitrogen metabolism[17]. We

82 designed an experiment to investigate the effect of glutamine auxotrophy on the metabolic

83 behavior of the organism under two pH conditions by comparing the results to those of the

84 wildtype[18]. For this purpose, a previously published genome-scale metabolic model[19] of the

85 wildtype was adjusted to represent the Δ*glnA* mutant. Experimental data of the Δ*glnA* mutant

86 was then used to constrain the solution space of the model. The results were compared with

87 a likewise constrained wildtype model, thereby providing an integrative view on the metabolic

88 adjustments that the organism has to perform to react to the imposed glutamine auxotrophy

89 during environmental pH changes.

90

91 Materials and Methods

92

93 Experimental

94 **Bacterial strains and culture conditions**

95 *Enterococcus faecalis* V583 Δ*glnA*[19] mutant was grown in batch cultures at 37 °C in a

96 chemically defined medium for lactic acid bacteria (CDM-LAB[13], pH 7.5 and 6.5). The CDM-LAB

97 medium contained the following per liter: 1 g K_2HPO_4, 5 g KH_2PO_4, $NaHCO_3$, 0.6 g ammonium

3

98   citrate, 1 g acetate, 0.25 g tyrosine,0.24 g alanine, 0.5 g arginine, 0.42 g aspartic acid, 0.13 g

99   cysteine, 0.5 g glutamic acid, 0.15 g histidine, 0.21 g isoleucine, 0.475 g leucine, 0.44 g lysine,

100   0.275 g phenylalanine, 0.675 g proline, 0.34 g serine, 0.225 g threonine, 0.05 g tryptophan,

101   0.325 g valine, 0.175 g glycine, 0.125 g methionine, 0.1 g asparagine, 0.2 g glutamine, 10 g

102   glucose, 0.5 g L-ascorbic acid, 35 mg adenine sulfate, 27 mg guanine, 22 mg uracil, 50 mg

103   cystine, 50 mg xanthine, 2.5 mg D-biotin, 1 mg vitamin B12, 1 mg riboflavin, 5 mg

104   pyridoxamine-HCl, 10 mg p-aminobenzoicacid, 1 mg pantothenate, 5 mg inosine, 1 mg

105   nicotinic acid, 5 mg orotic acid, 2 mg pyridoxine, 1 mg thiamine, 2.5 mg lipoic acid, 5 mg

106   thymidine, 200 mg $MgCl_2$, 50 mg $CaCl_2$, 16 mg $MnCl_2$, 3 mg $FeCl_3$, 5 mg $FeCl_2$, 5 mg $ZnSO_4$, 2.5

107   mg $CoSO_4$, 2.5 mg $CuSO_4$, and 2.5 mg $(NH4)_6Mo_7O_{24}$.

108

109   **pH shift experiments in chemostat cultures**

110   The pH shift experiments were carried out as previously described[18]. In short, *E. faecalis* V583

111   Δ*glnA* was grown in glucose-limited chemostat cultures in Biostat B Plus benchtop bioreactors

112   (Sartorius) in 750 ml CDM-LAB with a dilution rate of 0.15/h at 37 °C and gassing with 0.05

113   L/min nitrogen and stirring with 250 rpm. The pH was kept at the desired level by titrating

114   with 2 M KOH. Initially, the pH was kept constant at 7.5 until a steady state was reached.

115   Steady state was assumed when no glucose was detectable in the culture supernatant

116   anymore and dry mass and optical density (600 nm) were constant on two consecutive days.

117   For the pH shift, the pH control was switched off until the desired pH (6.5) value was reached.

118   The cultivation was continued until the steady-state was reached again. Samples were taken

119   at steady state pH 7.5 and at several time points during and after the pH shift as indicated in

120   Figure 1. Per sampling point, samples for determination of dry mass, extracellular metabolites

121   and proteomic analysis were taken as previously described[18].

122

123   **Chemostat cultures for determination of ATP$_{maintenance}$**

124   For determination of ATP$_{maintenance}$ (ATPm), *Enterococcus faecalis* V583 Δ*glnA* was grown in

125   glucose-limited chemostats as described above (except for pH shift) at two different dilution

126   rates, 0.15 h^{-1} and 0.05 h^{-1}, with three biological replicates per dilution rate. At steady-state

127   samples were taken and processed as described above.

128

129   **Quantification of extracellular metabolites**

4

130   For samples from pH shift experiments, quantification of amino acids in media and culture

131   supernatants was done by Frank Gutjahr Chromotgraphie (Balingen, Germany) and

132   quantification of lactate, formate, acetate, glucose, acetoin, 2,3-butanediol, ascorbate,

133   citrate, pyruvate and ethanol were done by Metabolomics Discoveries GmbH (Potsdam,

134   Germany). For quantification of amino acids, glucose, and fermentation products in CDM-LAB

135   and culture supernatants of samples from $ATP_{maintanance}$ experiments, the following two

136   methods were used:

137   Method 1: an Agilent 1260 Infinity II HPLC system was used. The system was controlled by

138   OpenLAB CDS Workstation software. For the amino acids analysis, sample supernatants were

139   filtered through a 0.22 µm syringe filter into a HPLC sample vial. Amino acids were derivatized,

140   separated on a reversed-phase column (Agilent Poroshell 120 EC-C18 4.6x100mm, 2.7µm),

141   detected with a diode array detector (DAD G7117A) and quantified following manufacturer's

142   guidelines (AdvanceBio Amino Acid Analysis, © Agilent Technologies, Inc. 2018). Standards

143   ranging from 5 µM to 30 mM were used for the quantification of aspartate, glutamate,

144   asparagine, serine, glutamine, histidine, glycine, threonine, arginine, alanine, tyrosine, valine,

145   methionine, tryptophan, phenylalanine, isoleucine, leucine, lysine and proline.

146   For analysis of organic compounds, samples were prepared as follows: 100 µl 35 % perchloric

147   acid were added to 1 ml sample, mixed and placed on melting ice for 10 minutes.

148   Subsequently, 55 µl potassium hydroxide solution (7 M) were added and the sample was

149   centrifuged for 2 min at 20,000 g. The supernatant was filtered through a 0.22 µm syringe

150   filter into a HPLC sample vial. Separation of sugars and fermentation products in the sample

151   was performed by using an Agilent Hi-Plex H column (4.6x250 mm, 8 µm) with a working

152   temperature of 65 °C using 10 mM H_2SO_4 as a mobile phase with a flow rate of 0.4 ml/min.

153   For detection, a refraction index detector (RID) with a working temperature of 35 °C and a

154   diode array detector (DAD) with a wavelength of 210nm/4nm with a reference wavelength of

155   360nm/100nm were used. Standards ranging from 50 µM to 150 mM were used for the

156   quantification of glucose, ethanol, citrate, lactate, pyruvate, formate and acetate.

157   Method 2: Sugars and organic acids in the supernatant were measured with an isocratic

158   Agilent 1200 series HPLC system equipped with a Phenomenex guard carbo-H column (4 by

159   3.0 mm) and a Rezex ROA organic acid H (8%) column (300 by 7.8 mm, 8 µm; Phenomenex)

160   maintained at 50°C. Analytes were separated and detected using 5 mM H2SO4 with a constant

161   flow rate of 0.4 mL min⁻¹. Prior to analysis samples were pretreated for precipitation of

5

162 abundant phosphate by addition of 4 M NH3 and 1.2 M MgSO4 solution followed by

163 incubation with 0.1 M H2SO4. Absolute concentrations were obtained by standard-based

164 external calibration and normalization with L-rhamnose as internal standard.

165

166 **Quantification of protein abundances**

167 All the steps in quantification of protein abundances were exactly carried out as previously

168 described in Großeholz *et al*[18].

169

170 Computational

171 **Determination of non-growth associated ATP$_{maintenance}$**

172 The determination of non-growth associated ATP (ATPm) was performed as described in

173 Teusink et. al[20]. Thus, the measured flux value for the carbohydrates, organic acids and amino

174 acids were integrated in the genome-scale model as constraints. The biomass reaction was

175 fixed at the respective growth rate (dilution rate) and the flux of the ATPm reaction was

176 maximized as the objective function. The obtained values were used to fit a linear function,

177 for which the *y*-intercept determines the required energy for the organism at zero growth

178 rate. This value is then applied to the model as the lower bound of the ATPm reaction.

179

180 **Integration of constraints to the genome-scale model**

181 The integration of constrains to the genome-scale model were done as indicated in Großeholz

182 *et al*[18]. To integrate the metabolic data a tolerance level of 40% was applied to the measured

183 flux rates to account for measurement errors. The obtained values were applied to the upper

184 (+ 20%) and lower (-20%) bounds of the respective exchange reactions at both conditions.

185 Regarding the proteome data, the reaction with no experimental evidence at the proteome

186 level at pH 7.5 were deactivated. To represent the significant fold changes of proteins in

187 response to pH shift, the log2 change of protein abundances were multiplied by 40%

188 (tolerance level) and then applied to the maximum and minimum value of respective

189 reactions, obtained by flux variability analysis (FVA)[21] at pH 7.5.

190

191 Results

192 In order to follow the metabolic adjustments to pH changes in the Δ*glnA* mutant of *E. faecalis*

193 V583 a chemostat set-up was used and a pH shift from pH 7.5 to 6.5 was applied. The

6

194   respective pH profile can be seen in Fig. 1. At all indicated time-points, samples were taken

195   and subjected to biomass, metabolite and proteome measurements. The results are

196   compared with earlier measurements of the corresponding *E. faecalis* wildtype strain under

197   the same conditions[18].

198
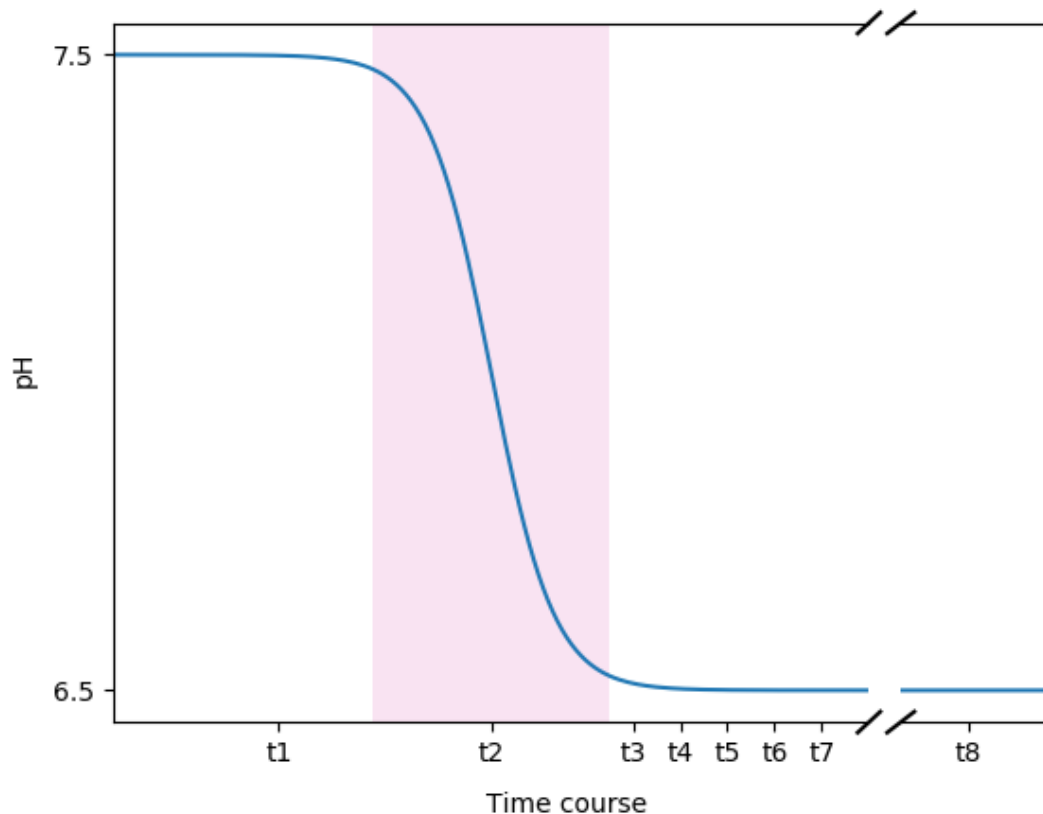
199   *Figure 1. Time course of the pH shift experiment. Samples were taken at t1 (steady-state at pH*

200   *7.5), t2 (the transition state (pink background) during the pH shift), t3, t4, t5, t6 and t7 which*

201   *indicate data points at pH 6.5 at 80, 100, 120, 180 and 240 minutes after the start of the pH*

202   *shift. Finally, samples were taken at t8, the steady-state at pH 6.5, 21 h after the start of the*

203   *experiment. The distance between the data points does not represent the actual time*

204   *difference in the experiment. Also, the break between t7 and t8 shows the shortened x axis*

205   *between the two data points.*

206

207   Effect of pH on the growth rate

208

209   The biomass production of *E. faecalis* Δ*glnA* decreased from 1.54 to 1.15 g/l when the pH was

210   shifted from 7.5 to 6.5 (Fig. 2). The trend of decreasing the biomass production at lower pH

211   values is similar to the wildtype, as the biomass production in both genotypes decreased by

7

212   approximately 25% in response to pH shift. However, the biomass production of the wildtype

213   at any given pH value is larger than that of the mutant, suggesting an important role of the

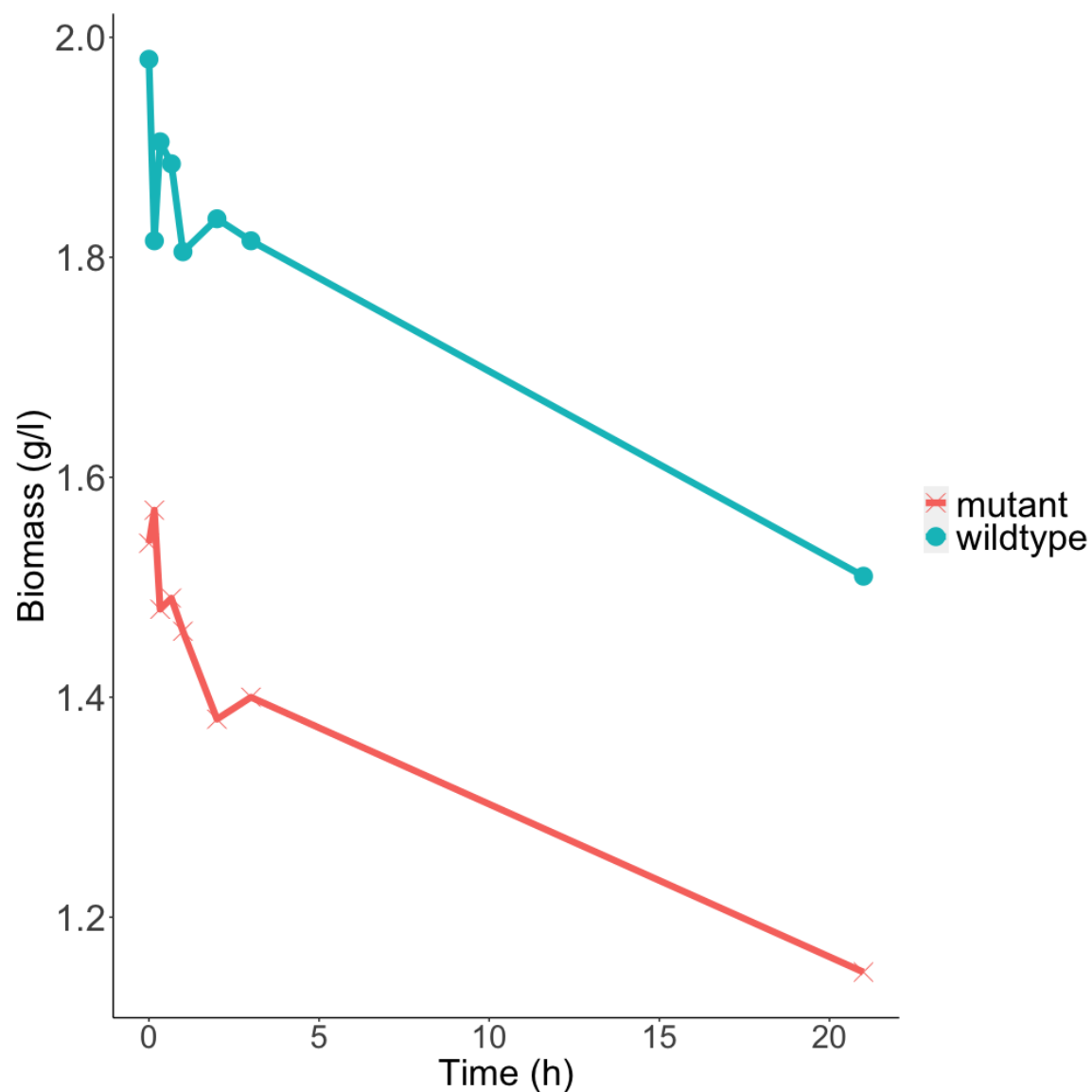214   glutamine synthetase reaction for the growth of the organism.

215

Figure 2. Development of the biomass production over the course of 21 hours during the pH

217   *shift experiment. The red line shows the biomass values of the E. faecalis Δglna mutant, while*

218   *the blue line shows the one of the wildtype. Each data point represents the mean of two*

219   *biological replicates.*

220

221   The effect of pH on metabolite uptake and production

222

223   To discover the effect of a pH shift on the metabolic behavior of *E. faecalis ΔglnA,* the

224   concentration of the extracellular carbon source (glucose), organic acids as well as amino acids

8

225   was determined in the samples of the chemostat experiment and the respective uptake or

226   production rates were calculated accordingly (Fig. 3). The measured profile of the carbon

227   source and organic acids consists of the uptake rate of glucose, as the primary energy source

228   for the organism, and the fermentation profile containing lactate, acetate, ethanol and

229   formate, reflecting the state of the energy metabolism at each pH value. Similar to the

230   wildtype, the glucose uptake rate increased in response to the drop in pH, indicating a higher

231   energy demand in a more acidic environment. This is mostly caused by the need to pump

232   protons out of the cell at the expense of ATP[18]. Moreover, and also similar to the wildtype,

233   the fermentation pattern changed from mixed acid fermentation to homolactic fermentation,

234   as homolactic fermentation is energetically more favorable. Despite the qualitative similarity

235   of the pH response to that of the wildtype, quantitatively, the uptake rate of glucose in the

236   mutant showed a stronger increase compared to the wildtype. This is translated to a higher

237   lactate production, suggesting a higher energy demand in response to pH shift in the Δ*glnA*

238   mutant. Also, the extent of shift to homolactic fermentation is stronger in the mutant. So, in

239   summary, these results indicate a higher energy demand in the Δ*glnA* mutant of *E. faecalis*

240   compared to the wildtype at all pH values.

241

242   This increased energy demand is also suggested when comparing the uptake and production

243   rates of amino acids between *E. faecalis* Δ*glnA* and the wildtype (Fig. 4). Overall, the amino

244   acids uptake rate decreased in response to pH shift with the exception of arginine, glutamine

245   and serine. Since less biomass is produced and more ATP is needed for proton export, less

246   protein synthesis should occur. At the same time, amino acid uptake is also energy consuming

247   since it is accompanied by either direct ATP consumption or additional proton import.

248   Therefore, it is interesting to look at the reason for an increased uptake rate under these

249   conditions. The uptake rate of arginine and serine, as well as the production rate of ornithine

250   both increased in the wildtype and the mutant after the pH shift. It has been reported that

251   the catabolism of arginine via arginine deaminase is used by a variety of lactic acid bacteria in

252   response to a more acidic environment[22]. Initially, it had been believed that there is a

253   beneficial buffering by ammonia. But when calculating the actual stoichiometries, we

254   previously showed that this is not the case at the respective pH[13]. However, arginine is readily

255   metabolized to gain ATP which can be used to pump protons to the extracellular environment

256   under a more acidic condition. Therefore, it can be suggested that under more energy-

257 demanding conditions (mutant versus wildtype, and pH 6.5 versus 7.5 (in both genotypes)), a

258 higher uptake rate of arginine may help cells to boost energy production. Serine uptake was

259 also increased after the pH shift in the ΔglnA mutant, as serine can as well be used for ATP

260 production via degradation to ammonia and pyruvate and fermenting pyruvate to acetate.

261 Additionally, the uptake rate of glutamine and the production rate of ammonia were

262 considerably higher in the mutant compared to the wildtype at both pH levels. The latter is a

263 curious observation, since the export of such amounts of ammonia points to excess nitrogen

264 from glutamine. The glutamine auxotrophy of the mutant might explain the larger margin

265 between the two pH values, as the higher uptake rate ensures that the growth is less affected

266 by the auxotrophy. More importantly, however, it has been reported that in *Streptococcus*

267 *pneumoniae*[23] the transcription factor GlnR (which controls the production and transport of

268 glutamine) is dependent on the intact gene for GlnA to successfully function. The

269 overproduction of ammonia suggests that the regulatory effect of GlnR is also disrupted in *E.*

270 *faecalis ΔglnA*, resulting in the upregulation of the glutamine ABC transporter (GLNabc) and

271 an unnecessarily high glutamine uptake rate accordingly. This also accounts for the small

272 glutamate excretion in the mutant at pH 6.5, since massive amounts of glutamine will drive

273 the glutamine deaminase to produce both glutamate and ammonium. The glutamate

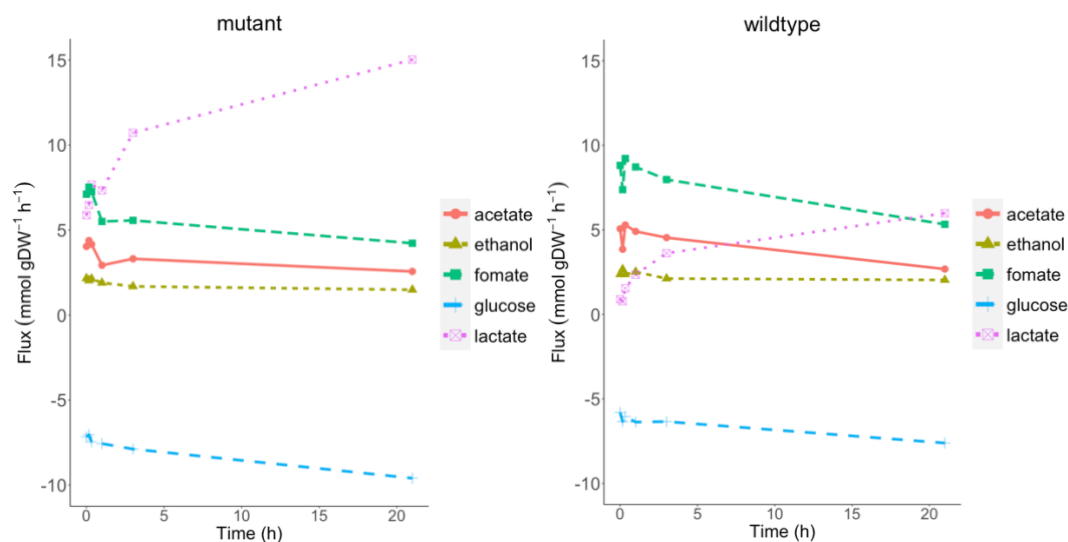274 excretion was however not observed in a previous study[19].

275

276 *Figure 3. The uptake and production rate of glucose and fermentation products during the pH*

277 *shift experiment. The left panel shows the data from the mutant, and the right panel shows*

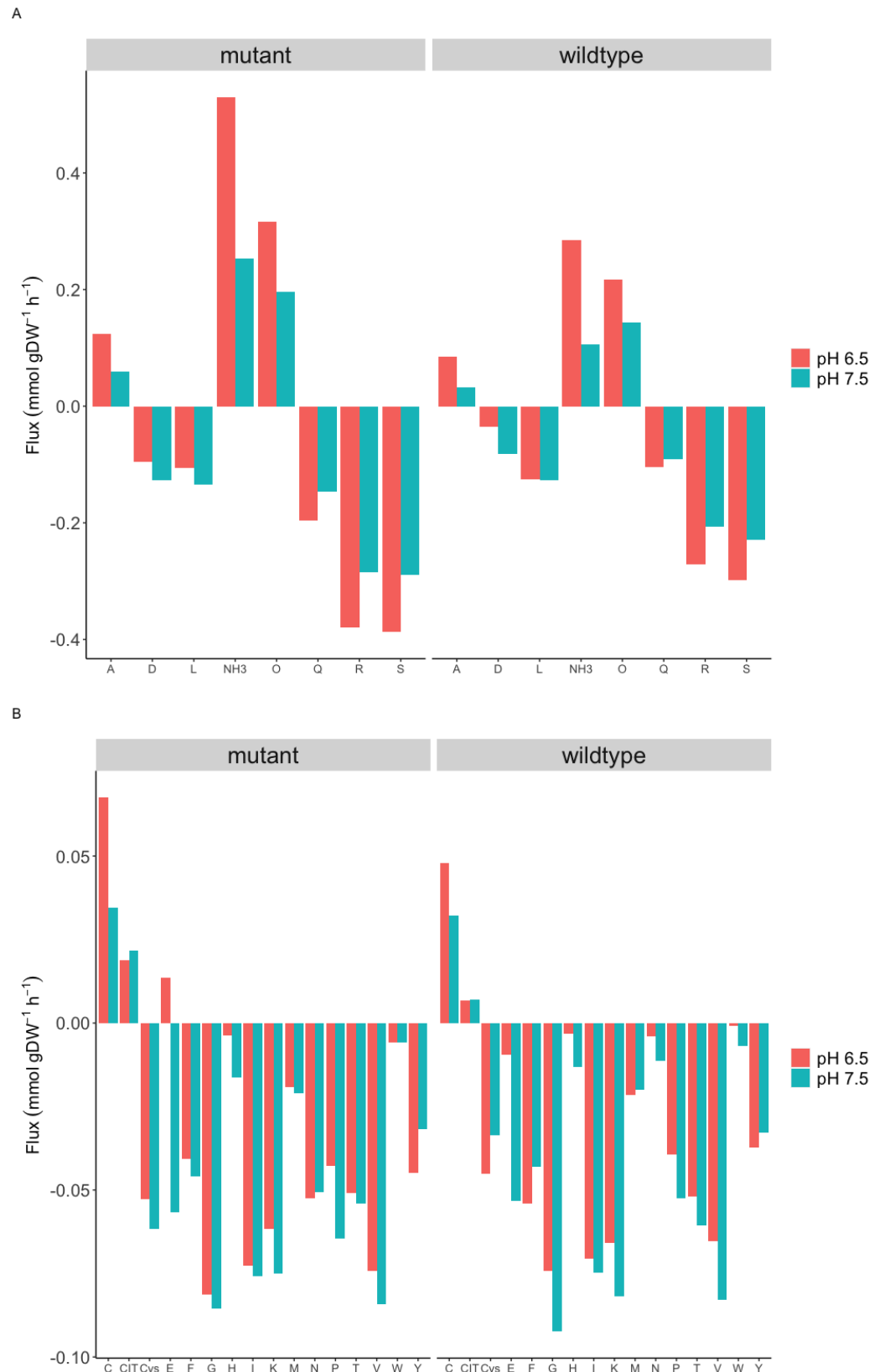278 *the data from the wildtype. Each data point represents the mean of two biological replicates.*

279

280

281

282 *Figure 4. The uptake and production of the amino acids in the wildtype and the ΔglnA mutant*

283 *at pH 7.5 and 6.5 (t1 and t8, respectively). Panel A shows the uptake/production rate of amino*

284 *acids with high flux value (larger than 0.1 mmol/g$^{-1}_{DW}$h^{-1}) and panel B shows the*

285 *uptake/production rate of amino acids with low flux value (smaller than 0. mmol/g$^{-1}_{DW}$h^{-1})*

286   Significant fold changes on protein level during the pH shift

287

288   To observe the effect of the pH shift on the protein expression in *E. faecalis ΔglnA,* the

289   expression rate of all detected proteins was quantified throughout the pH shift experiment

290   and the respective significant fold changes were calculated at different time points compared

291   to time point 1 (t1). The complete set of significantly changed protein expressions is shown in

292   the supplement (supplementary table 1). While there was no significant fold change at t2, the

293   highest number of fold changes was observed at t3, 20 minutes after the start of the pH shift,

294   with more than 40 proteins (out of 1681 detected ORFs) being affected. Among all affected

295   proteins eleven are involved in membrane and cell wall production, and two proteins assigned

296   to reactions involved in peptidoglycan biosynthesis. This suggests that restructuring of the

297   membrane and cell envelope occurs early in response to a change in environmental pH -

298   similar to what has been observed for the wildtype[18]. A smaller number of proteins was

299   affected by the pH shift between t4 (1 hour after start of the pH shift) and t7 (4 hours after

300   start of the pH shift), all of which were downregulated. At t8, 21 hours after the pH shift, the

301   number of significant fold changes amounted to 40, with the majority of the proteins being

302   downregulated. A large number of these is involved in nucleotide biosynthesis (Table 1).

303   Considering the fact that *de novo* biosynthesis of nucleotides is an energy demanding process

304   for the organism, the down regulation of the respective pathways is in line with the higher

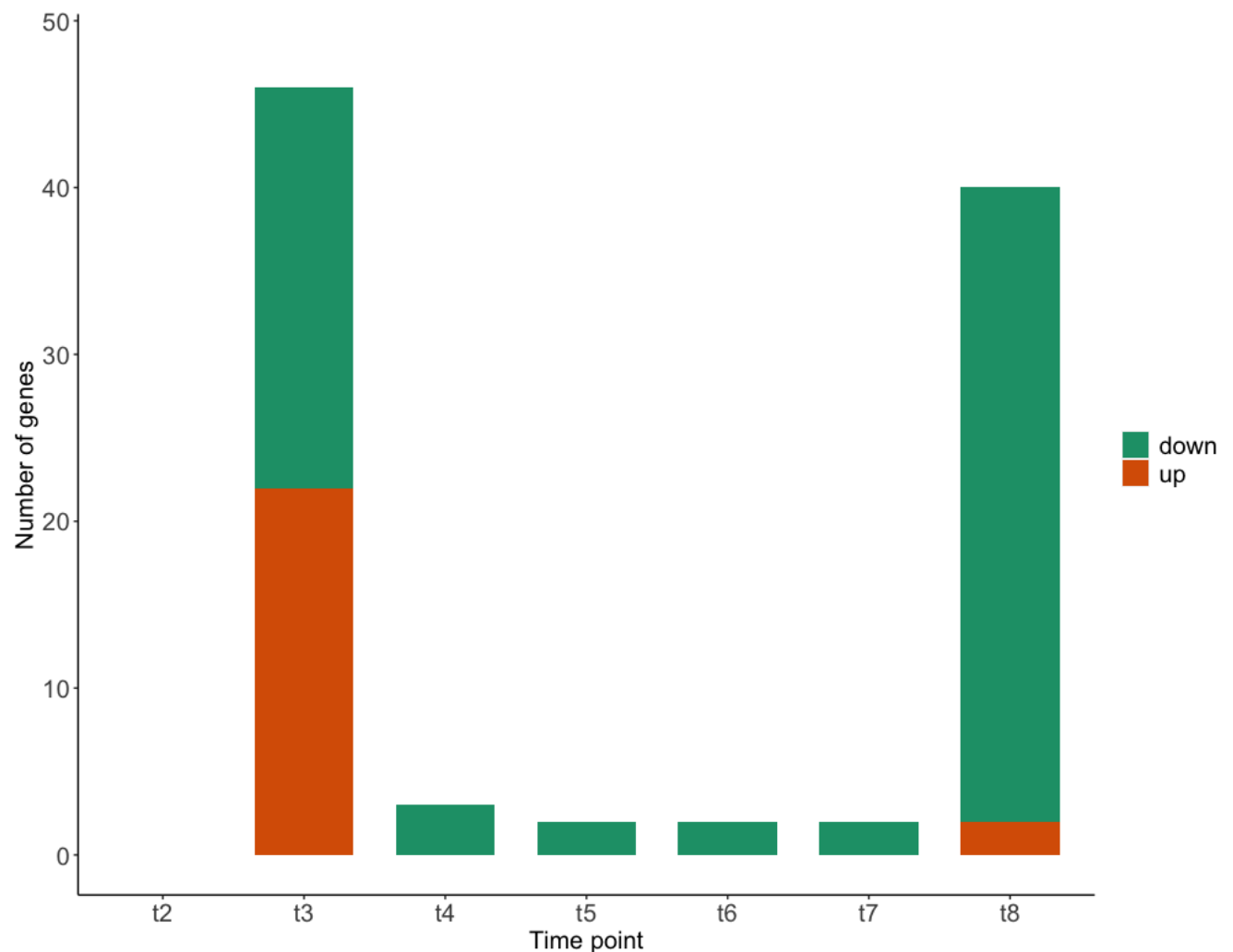305   energy demand under the more acidic condition.

306

307

12

Figure 5. The significant change in protein abundances in the ΔglnA mutant during the pH shift experiment at different time points.

To find out the differences between the wildtype and the mutant at the proteome level in response to pH shift, the significant fold changes were compared. Except for t8, the number of significant fold changes in the wildtype was considerably higher than that in the mutant. As already mentioned, at early time-points, both the mutant and the wildtype showed fold changes in enzymes that are involved in membrane and cell wall production. However, at these early time-points after pH shift the wildtype also displayed an upregulation of glycolytic enzymes compared to the mutant. The lack of increased expression in glycolytic enzymes in the mutant might be explained by the previously introduced higher energy demand. Since glycolysis is responsible for the major energy production in *E. faecalis*, it is plausible that the expression of those enzymes was already at a higher level in the mutant. The downregulation

13

322   of enzymes involved in nucleotide metabolism after the pH-shift is again similar between

323   wildtype and mutant.

324

325

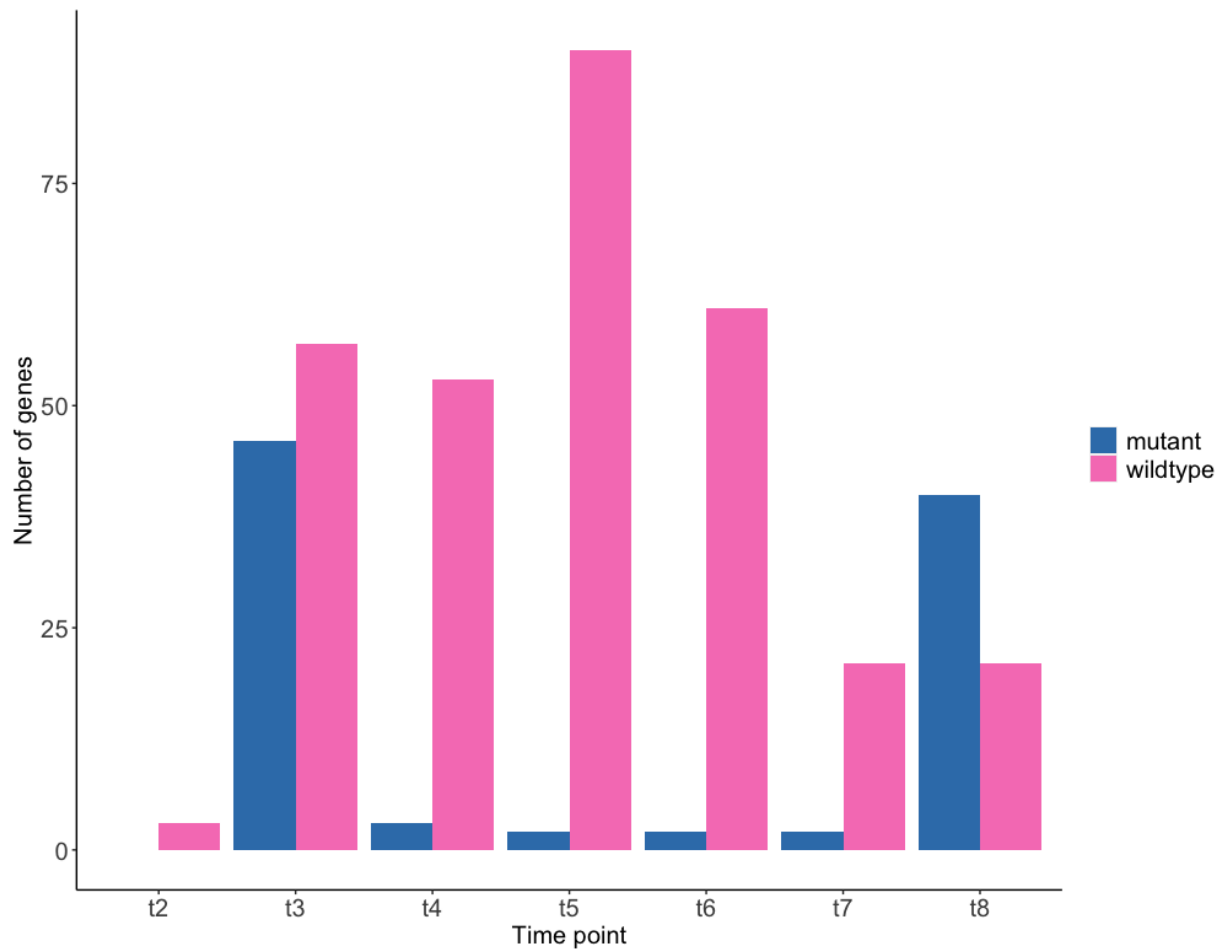*Figure 6. The number of significant changes in protein abundances during the pH shift experiment in the wildtype and the ΔglnA mutant.*

Table 1. The number of significant changes in protein abundances and the prominent respective subsystems at t8 (ΔglnA mutant)

Subsystems	Number of affected genes
Amino acid metabolism	3
Carbohydrate metabolism	7
Nucleotide metabolism	22
Transport	6

330

331   Computational

332   In order to study the metabolic behavior of *E. faecalis* ΔglnA more comprehensively and on a

333   cell-wide scale, genome-scale modelling in combination with constraint-based modelling was

14

334   applied. For that matter, the previously published genome-scale metabolic network of *E.*

335   *faecalis*[19] was used to simulate the pH shift experiment by the integration of metabolic and

336   proteomic data from the *E. faecalis ΔglnA*. To integrate the experimental data into the

337   genome-scale model, the framework from our previous[18] work was applied. To represent the

338   *glnA* knock-out in the model, the reaction flux of glutamine synthetase was set to zero. The

339   complete model is available at biomodels.

340

341   Determination of the non-growth associated ATP value of *E. faecalis ΔglnA*

342

343   In order to prepare the genome-scale model of *E. faecalis ΔglnA* for the integration of the

344   above described data and the analysis via FBA, we determined the non-growth associated

345   energy demand (ATPm) which is an important feature for performing FBAs. The non-growth

346   associated energy demand reflects the amount of energy required to sustain life at zero

347   growth. Thus, the definition of this parameter is an important aspect for genome-scale

348   modelling as it can strongly affect the flux distributions in the metabolic network.

349   For this purpose, *E. faecalis ΔglnA* was grown in chemostat cultures at two different dilution

350   rates (0.05, 0.15 h^{-1}). After reaching the steady-state, samples were taken from the chemostat

351   cultures and the metabolite composition in the supernatant was experimentally determined

352   to calculate the uptake/production rate of extracellular metabolites (Table 2). The uptake and

353   production rates of glucose, organic acids, and amino acids were then integrated into the

354   model as reaction constraints, defined as bounds on the respective exchange reactions. To

355   calculate parameters for the ATPm reaction, for each dilution rate, the biomass production

356   reaction was fixed at the maximal growth rate that is equal to the value of the dilution rate,

357   and the flux through the ATPm reaction was maximized as the new objective function. The

358   obtained maximal objective function value, namely the maximal flux through the ATPm

359   reaction at different dilution rates is plotted against the respective dilution rate and a linear

360   function was fitted to those values. The non-growth associated energy reflects the amount of

361   energy that microbes require to survive at zero growth and is derived from the *y*-intercept of

362   the linear function. This value represents the maintenance energy and was used as the lower

363   bound of the ATPm reaction in the model.

364   This constraint ensures that the minimum required amount of energy for non-growth

365   associated purposes is produced by the model and is not channeled into biomass production

15

366 and thus into growth. As a result, the calculated value of ATPm of the *E. faecalis* Δ*glnA* was

367 5.977 and 6.224 mmol/g$^{-1}_{DW}$h^{-1} at pH 7.5 and 6.5, respectively. When integrated into the

368 model, however, the maximal biomass production is too high compared to experimental data.

369 In fact, the level at which the model produced the fermentation products resulted in a very

370 high ATP production, so at this value of ATPm, the ATP is redirected into biomass production.

371 Hence, the constraints of this reaction had to be set on a higher value under both pH

372 conditions. Several reasons allow for such adjustment without violating the modeling rules.

373 First, the ATPm is an estimated value by taking the measured value of around 30 metabolites

374 into account. Therefore, the estimation is very error prone, as the measurement error of all

375 the metabolites accumulate and impact the optimization process. For instance, the glucose

376 uptake rate at pH 7.5 at the dilution rate of 0.15 was 6.32 mmol/g$^{-1}_{DW}$h^{-1} in the data set used

377 for ATPm estimation, and 7.17 mmol/g$^{-1}_{DW}$h^{-1} in another previously measured data set shown

378 in Figure 3. This difference of 0.85 mmol/g$^{-1}_{DW}$h^{-1} results in approximately 2 mmol/g$^{-1}_{DW}$h^{-1}

379 difference at the optimized ATPm value at this particular condition. Second, the ATPm value

380 in essence is meant to ensure that the model is not reaching the optimal growth by

381 overlooking the non-growth associated energy. In this sense, deviation from the estimated

382 value to a higher value does not violate the underlying assumption, while deviation to a lower

383 value would require more solid evidence. Here, both calculated values for the ATPm reaction

384 seem to be too low and had to be increased. If we consider lactate production as an indicator

385 of the energetic state of the cell, the fact that the lactate production in the mutant is several

386 times higher than in the wildtype suggests a much higher ATPm value for the mutant

387 compared to the wildtype (the ATPm values in the wildtype were calculated to be 3.9 mmol/g$^{-1}_{DW}$h^{-1}

388 at pH 7.5 and 8.4 mmol/g$^{-1}_{DW}$h^{-1} at pH 6.5[18]). Therefore, the ATPm values in the mutant

389 were increased to 9.7 mmol/g$^{-1}_{DW}$h^{-1} and 10.6 mmol/g$^{-1}_{DW}$h^{-1} at pH 7.5 and 6.5, respectively.

390 For pH 7.5, this represents the minimal value for the correct reproduction of biomass

391 production. For pH 6.5 we selected a higher value, but noted that the exact value does not

392 considerably impact the solution. These values allowed for a precise prediction of the biomass

393 and the production rates of the organic acids. It is necessary to point out that under both pH

394 conditions, in addition to being glucose limited, the chemostat cultures were also deprived of

395 glutamine, suggesting that the glutamine content of the CDM-LAB might be limiting and might

396 thus be insufficient to fulfill the demands in *E. faecalis* Δ*glnA.*

397

16

398   Predicted flux through the energy metabolism in the Δ*glnA* mutant

399

400   The experimentally measured metabolic and proteomic data were integrated into the Δ*glnA*

401   genome-scale model to simulate the pH shift experiment (as described for the wildtype[18]).

402   Thus, in short, the uptake and release fluxes are set as boundaries for the respective fluxes

403   and fluxes associated with proteins not present in the proteome data are set to zero, if not

404   essential. Finally, adjustments of fluxbounds according to de- or increases in expression are

405   implemented.

406

407   As reflected by the experimental data, the Δ*glnA* mutant has a higher energy demand at all

408   conditions. This obviously also holds true in the model after the integration of experimental

409   data. The model shows an increased flux through glycolysis, which implies a higher ATP

410   production. Accordingly, the predicted flux through lactate dehydrogenase (LDH) is also

411   increased after the pH shift.

412

413   The flux distribution in glycolysis was compared between wildtype and mutant to investigate

414   the difference in flux values in energy metabolism. At pH 7.5 a higher flux value passed

415   through the glycolytic reactions in the mutant as a result of the higher energy demand. In the

416   model, the higher energy demand in the mutant results from the need to import glutamine

417   from the extracellular environment either via the GLNabc (glutamine ATP binding cassette)

418   transporter or via glutamine permease. GLNabc-mediated uptake of glutamine consumes ATP

419   and permease-mediated uptake imports protons into the cell, which subsequently increases

420   the ATP demand as ATP is required to pump protons out of the cell. However, glutamine

421   synthesis from glutamate would of course also consume one ATP per glutamine. Therefore,

422   the striking difference in energy demand is still not explained. We will come back to this point

423   below.

424

425   Impact of glutamine uptake in the model of *E. faecalis* Δ*glnA*

426

427   As explained above, the fact that the Δ*glnA* mutant is unable to produce glutamine leads to

428   increased uptake of extracellular glutamine. Based on the chemostat data, glutamine uptake

429   increased from t1 at pH 7.5 to time point 8 at pH 6.5, corresponding to a 34% increase from

430   0.147 mmol/g$^{-1}_{DW}$h^{-1} to 0.197 mmol/g$^{-1}_{DW}$h^{-1}, respectively. Originally, the glutamine transport

17

431   via the glutamine ABC transporter (R_GLNabc) and glutamine permease (R_Glnt6) were

432   represented in the model. As proteome data suggested, the ATP binding subunit of the

433   GLNabc (EF0760) was upregulated after the pH shift, suggesting an increase of the transporter

434   demand which is consistent with the higher uptake rate of glutamine. Considering the fact

435   that membrane proteins were often missing from the proteomic data set (due to technical

436   issues), it is likely that the other subunits of the transporter were subjected to upregulation

437   as well, as there is an increase in glutamine uptake after the pH shift. However, the original

438   design of the glutamine transport in the model could not translate the upregulation of GLNabc

439   into a higher flux. The FBA flux distribution revealed a flux value of zero for GLNabc under both

440   pH conditions. In order to gain a consistent result between the model and the experimental

441   data, an improved, new permease reaction was introduced to the model. As reported

442   previously, the permease system in *E. faecalis* is not amino acid-specific, but is rather shared

443   between multiple amino acids with various affinities[24]. It is suggested that while glutamine

444   has the highest affinity to the transporter, the same transporter takes up asparagine and

445   threonine as well. Hence, to account for the higher affinity of the transporter for glutamine

446   compared to the other amino acids, the new permease reaction in the model was designed to

447   carry two glutamines together with one asparagine and one threonine and four protons (one

448   per each amino acid molecule). The previous amino acid specific permease of all three amino

449   acids were then deactivated accordingly. The new transport design resulted in a successful

450   prediction of the uptake rate of all three amino acids and also in using GLNabc when a higher

451   uptake rate is in demand after the pH shift. The new set up accounts for the actual transport

452   system in a more accurate way, as it mimics the shared permease system and also gets the

453   ABC transporter in use when needed. The fact that during glutamine uptake involuntarily and

454   automatically other amino acids are taken up as well (expending ATP or taking up protons)

455   might be also at least partially the source for the high energy demand of the mutant. In

456   addition, and as mentioned above, the regulatory effect of GlnR in *E. faecalis* Δ*glnA* might be

457   disrupted so that the uptake of glutamine (and the other amino acids transported by the same

458   proteins) is less strictly regulated.

459

460   Predicted flux through glutamine/glutamate metabolism

461

462   The flux distribution of the genome-scale model was subsequently used to analyze the effect

463   of the pH shift on glutamine-glutamate metabolism. This pathway is of particular interest as

464   we aimed to uncover the consequences of glutamine auxotrophy in the metabolism of *E.*

465   *faecalis* in this study. Following an increase in glutamine uptake and on the contrary, decrease

466   in glutamate uptake, the model predicted an upregulation in the glutamine to glutamate

467   conversion, which was reflected in switching on the two reactions, aspartyl-tRNA(Asn):L-

468   glutamine amido-ligase (ADP-forming) (ASNTAL) and carbamoyl-phosphate synthase

469   (glutamine-hydrolysing) (CBPS). Interestingly, the model predicted a flux shutdown at

470   glutamine-fructose-6-phosphate (gam6p) transaminase, which produces glucose amine-6-

471   phosphate by a transaminase reaction between glutamine and fructose-6-phosphate. Instead,

472   gam6p is produced by assimilating ammonia into fructose-6-phosphate. The model also

473   predicted an increased flux towards the reverse direction of glutamate dehydrogenase (GDH),

474   producing glutamate from 2-oxoglutarate. The directionality of GDH plays an important role

475   in balancing the carbon and nitrogen metabolism[25]. The NADPH/NADP ratio is directly

476   influenced by less NADPH being available for e.g. amino acid biosynthesis when the flux is

477   directed towards glutamate production. This also coincides with our observation of a strongly

478   decreased uptake of glutamate from the medium and an increased uptake of glutamine

479   (which is required for 2-oxoglutarate production). The decreased level of NADPH also prevents

480   reductive synthesis reactions from taking place, as it is reflected in the significant

481   downregulation of proteins involved in e.g. nucleotide metabolism. As another beneficial side

482   effect, the reverse direction of the GDH consumes one proton. This flux change also leads to

483   a series of changes in other amino acid production/degradation processes. For instance, a

484   higher conversion rate of glutamate to alanine and aspartate was predicted, with the former

485   being excreted by the cell after the pH shift, based on the experimental data.

486

487   **Discussion**

488   *E. faecalis* is important in the food industry and hospital environments; therefore,

489   characterizing its highly adaptive metabolism is necessary. Hence, Integrative analysis of

490   bacterial metabolism is a key approach to uncover their adaptive behavior. In this study we

491   analyzed the effect of a decline in environmental pH from 7.5 to 6.5 on a *ΔglnA* mutant of *E.*

492   *faecalis* and compared the results to those of the wildtype[18]. Like the wildtype, the *ΔglnA*

493   mutant responded to the pH shift by reprogramming its metabolic and proteomic profile to fit

19

494   the increased energy demand that comes with the need to maintain a higher pH by pumping

495   protons out of the cell. Many findings therefore paralleled the results from the wildtype

496   thereby also confirming these. However, there are also striking differences, mostly concerning

497   the quantity of the energy demand in the genotypes.

498

499   Similar to the wildtype, the mutant decreased biomass production during pH shift since less

500   ATP is available for anabolic processes. In addition, there is a pronounced shift from mixed

501   acid to homolactic fermentation. While the qualitative pattern in the mutant resembled the

502   one in the wildtype, the proportion of lactate production in the mutant was considerably

503   higher. This confirms that under more energy-demanding conditions (*ΔglnA* mutant or acidic

504   conditions), *E. faecalis* changes its fermentation profile to homolactic fermentation. While the

505   stoichiometric analysis of the fermentation pathway shows that mixed acid fermentation

506   produces one more ATP, it is widely reported that LAB species such as *L. lactis* and *L.*

507   *plantarum* choose homolactic fermentation during high glycolytic flux, high substrate

508   availability or faster growth rates[26]. The high uptake rate of glucose under energetically

509   demanding conditions, which further translates into a higher glycolytic flux, increases the

510   NADH/NAD ratio. Reportedly, a higher ratio of NADH/NAD upregulates the activity of lactate

511   dehydrogenase (LDH), e.g. in *L. lactis*[27]. While this has been observed in the literature, a

512   plausible explanation why the less productive (in terms of ATP) fermentation is favored under

513   energetically demanding conditions is still missing.

514

515   The amino acid uptake/production profile further underlines the overwhelming influence of

516   the growing energy demand when pH is lowered. The uptake rate of amino acids mostly

517   decreased following the pH shift except for arginine, serine and glutamine. A decreased amino

518   acid uptake should be a result of regulation when less biomass is produced, and also saves

519   energy, since the uptake is either coupled to even more proton uptake or to ATP hydrolysis.

520   The increased uptake of arginine and serine can be easily explained since these can be directly

521   used for ATP production. Arginine is considered a prolific energy resource in many lactic acid

522   bacteria, especially those important in the food industry[28,29]. An interesting aspect of arginine

523   catabolism in lactic acid bacteria (when used for energy production) is that it often does not

524   result in citrulline production, regardless of using arginine deaminase or not[28,29]. Likewise, our

525   data suggested that an increase in arginine uptake following the pH shift leads to an increase

20

526 in ornithine, but not citrulline production. The previous finding on the production of ornithine

527 from citrulline through ornithine carbamoyl transferase in *E. faecalis*[30] was supported by the

528 flux distribution in the genome-scale model. Ornithine is then used by the arginine-ornithine

529 antiporter to import even more arginine into the cell.

530

531 Not surprisingly, there is quite a big difference between wildtype and mutant in

532 glutamine/glutamate metabolism and how this is affected by the pH shift. While the uptake

533 rate of glutamate considerably decreased in response to pH shift, the glutamine uptake rate

534 was increased – in the wildtype only very slightly and strongly in the mutant. As discussed

535 above, several mechanisms might contribute to this observation – first, we proposed in

536 accordance with literature on *S. pneumoniae*[23] that the regulatory effect of the transcription

537 factor GlnR on the uptake of glutamine depends on the intact gene for GlnA and its absence

538 results in an unregulated glutamine uptake. Second, the reversal of the flux of the GDH with

539 its regulatory consequences is only possible, if more 2-oxoglutarate is produced for which

540 glutamine is needed. Third, as learned from the genome-scale model, it is important to

541 consider the lack of specificity of the amino acid uptake mechanisms. Co-transported with e.g.

542 glutamate are amino acids like aspartate that cannot readily be catabolized for energy

543 production. In the case of glutamine, at least small amounts of arginine are also co-

544 transported which is favorable under high energy demand.

545

546 The glutamine synthetase reaction (catalyzed by GlnA) is the main reaction to assimilate

547 ammonium[17]. However, here glutamine is imported in such large quantities that some of it

548 has to be deaminated to produce glutamate (so that even a small amount of excretion is

549 observed) and ammonium which the model also predicted. Although high concentrations of

550 ammonium are reported to lower the growth rate in bacteria, the underlying reason is

551 suggested to be the general osmotic or ionic effect of ammonium rather than its toxicity[31].

552 The exact mechanism of ammonium export is not known, but likely either ask for proton

553 antiport or ATP which adds to the energy demand of the mutant.

554

555 The analysis of the proteome data again showed a lot of parallel adjustments to pH shift

556 between wildtype and mutant. Here, the decrease of expression in enzymes of the *de novo*

557 biosynthesis of nucleotides which is costly, and also the upregulation of enzymes involved in

558 the restructuring of the cell membrane and cell wall which is necessary while facing a drop in

559 extracellular pH level in order to decrease proton leak is common between the genotypes. The

560 mutant however shows a striking lack of increasing the protein expression of glycolytic

561 enzymes at the beginning of the pH shift experiment. Since there is already a high glycolytic

562 flux in the mutant at the start of the experiment, we assume that the respective changes in

563 core metabolism already happened at this point.

564

565 All experimental data were reproducible in the genome-scale model. However, the

566 stoichiometry of amino acid uptake reactions had to be adjusted to a realistic depiction of

567 their non-specificity. To the best of our knowledge, this has not considered in other genome-

568 scale models of bacteria so far.

569

570 Initially, when considering all of the above findings which mostly reflect the higher need for

571 energy in the mutant, it was not obvious why this higher need arises. Glutamine is the primary

572 nitrogen donor in bacterial cells. High levels of glutamine have to be maintained in order to

573 allow effective transfer of amino-groups[32]. This can be accomplished by its synthesis and

574 uptake in the wildtype or its uptake alone in the mutant. At first glance the energetic cost of

575 glutamine uptake is comparable compared to its biosynthesis via GlnA. One ATP is needed for

576 GlnA and the usage of one ATP or proton import is the consequence of glutamine import.

577 However, if the control over glutamine uptake is inhibited due to the lack of GlnA, the

578 potentially uncontrolled and excessive import of glutamine may incur additional cost to the

579 cells. Thus, both the automatic co-transport of unwanted amino acids, as well as the need to

580 excrete large amounts of ammonia are certainly costly.

581

587

588 1.   F., H. J. *et al.* Enterococcus faecalis 6-Phosphogluconolactonase Is Required for Both

589   Commensal and Pathogenic Interactions with Manduca sexta. *Infect. Immun.* **83**, 396–

22

590   404 (2015).

591   2.   Hancock, L. E., Murray, B. E. & Sillanpää, J. Enterococci: From Commensals to Leading

592   Causes of Drug Resistant Infection. *Enterococcal Cell Wall Components Struct.* 1–35

593   (2014).

594   3.   Jabbari Shiadeh, S. M., Pormohammad, A., Hashemi, A. & Lak, P. Global prevalence of

595   antibiotic resistance in blood-isolated Enterococcus faecalis and Enterococcus

596   faecium: a systematic review and meta-analysis. *Infect. Drug Resist.* **12**, 2713–2725

597   (2019).

598   4.   Asadollahi, P., Razavi, S., Asadollahi, K., Pourshafie, M. R. & Talebi, M. Rise of

599   antibiotic resistance in clinical enterococcal isolates during 2001-2016 in Iran: a

600   review. *New microbes new Infect.* **26**, 92–99 (2018).

601   5.   L., K. A. *et al.* Enterococcus faecalis Tropism for the Kidneys in the Urinary Tract of

602   C57BL/6J Mice. *Infect. Immun.* **73**, 2461–2468 (2005).

603   6.   Dahlberg, A. C. & Kosikowsky, F. V. The Development of Flavor in American Cheddar

604   Cheese Made from Pasteurized Milk with Streptococcus Faecalis Starter[1].

605   *J. Dairy Sci.* **31**, 275–284 (1948).

606   7.   Fuller, R. Probiotics in man and animals. *J. Appl. Bacteriol.* **66**, 365–378 (1989).

607   8.   Baccouri, O. *et al.* Probiotic Potential and Safety Evaluation of Enterococcus faecalis

608   OB14 and OB15, Isolated From Traditional Tunisian Testouri Cheese and Rigouta,

609   Using Physiological and Genomic Analysis. *Front. Microbiol.* **10**, 881 (2019).

610   9.   Penkler, G. *et al.* Construction and validation of a detailed kinetic model of glycolysis

611   in Plasmodium falciparum. *FEBS J.* **282**, 1481–1511 (2015).

612   10.   Oberhardt, M. A., Palsson, B. Ø. & Papin, J. A. Applications of genome-scale metabolic

613   reconstructions. *Mol. Syst. Biol.* **5**, 320 (2009).

614   11.   Orth, J. D., Thiele, I. & Palsson, B. Ø. What is flux balance analysis? *Nat. Biotechnol.* **28**,

615   245 (2010).

616   12.   Bernstein, D. B., Sulheim, S., Almaas, E. & Segrè, D. Addressing uncertainty in genome-

617   scale metabolic model reconstruction and analysis. *Genome Biol.* **22**, 64 (2021).

618   13.   Levering, J. *et al.* Genome-scale reconstruction of the Streptococcus pyogenes M49

619   metabolic network reveals growth requirements and indicates potential drug targets.

620   *J. Biotechnol.* **232**, 25–37 (2016).

621   14.   Granata, I., Troiano, E., Sangiovanni, M. & Guarracino, M. R. Integration of

622   transcriptomic data in a genome-scale metabolic model to investigate the link

623   between obesity and breast cancer. *BMC Bioinformatics* **20**, 162 (2019).

624 15. Tian, M. & Reed, J. L. Integrating proteomic or transcriptomic data into metabolic

625   models using linear bound flux balance analysis. *Bioinformatics* **34**, 3882–3888 (2018).

626 16. Reed, J. L. Shrinking the Metabolic Solution Space Using Experimental Datasets. *PLOS*

627   *Comput. Biol.* **8**, e1002662 (2012).

628 17. Forchhammer, K. Glutamine signalling in bacteria. *Front. Biosci.* **12**, 358–370 (2007).

629 18. Großeholz, R. *et al.* Integrating highly quantitative proteomics and genome-scale

630   metabolic modeling to study pH adaptation in the human pathogen Enterococcus

631   faecalis. *Npj Syst. Biol. Appl.* **2**, 16017 (2016).

632 19. Veith, N. *et al.* Using a Genome-Scale Metabolic Model of Enterococcus faecalis V583

633   To Assess Amino Acid Uptake and Its Impact on Central Metabolism. *Appl. Environ.*

634   *Microbiol.* **81**, 1622 LP – 1633 (2015).

635 20. Teusink, B. *et al.* Analysis of Growth of Lactobacillus plantarum WCFS1 on a Complex

636   Medium Using a Genome-scale Metabolic Model*. *J. Biol. Chem.* **281**, 40041–40048

637   (2006).

638 21. Mahadevan, R. & Schilling, C. H. The effects of alternate optimal solutions in

639   constraint-based genome-scale metabolic models. *Metab. Eng.* **5**, 264–276 (2003).

640 22. Casiano-Colon, A. & Marquis, R. E. Role of the arginine deiminase system in protecting

641   oral bacteria and an enzymatic basis for acid tolerance. *Appl. Environ. Microbiol.* **54**,

642   1318–1324 (1988).

643 23. Kloosterman, T. G. *et al.* Regulation of Glutamine and Glutamate Metabolism by GlnR

644   and GlnA in Streptococcus pneumoniae*. *J. Biol. Chem.* **281**, 25097–25109 (2006).

645 24. Holden, J. T. & Bunch, J. M. Asparagine transport in Lactobacillus plantarum and

646   Streptococcus faecalis. *Biochim. Biophys. Acta - Biomembr.* **307**, 640–655 (1973).

647 25. Smith EL, Austen BM, B. K. & N. J. Glutamate dehydrogenases. *Enzym.* **11. (pp 29**,

648   (1975).

649 26. Teusink, B., Bachmann, H. & Molenaar, D. Systems biology of lactic acid bacteria: a

650   critical review. *Microb. Cell Fact.* **10**, S11 (2011).

651 27. Garrigues, C., Loubiere, P., Lindley, N. D. & Cocaign-Bousquet, M. Control of the shift

652   from homolactic acid to mixed-acid fermentation in Lactococcus lactis: predominant

653   role of the NADH/NAD+ ratio. *J. Bacteriol.* **179**, 5282–5287 (1997).

24

654   28.   Hwang, H. & Lee, J.-H. Characterization of Arginine Catabolism by Lactic Acid Bacteria

655   Isolated from Kimchi. *Molecules* **23**, 3049 (2018).

656   29.   Tonon, T. & Lonvaud-Funel, A. Metabolism of arginine and its positive effect on

657   growth and revival of Oenococcus oeni. *J. Appl. Microbiol.* **89**, 526–531 (2000).

658   30.   Knivett, V. A. The anaerobic interconversion of ornithine and citrulline by

659   Streptococcus faecalis. *Biochem. J.* **58**, 480–486 (1954).

660   31.   Müller, T., Walter, B., Wirtz, A. & Burkovski, A. Ammonium Toxicity in Bacteria. *Curr.*

661   *Microbiol.* **52**, 400–406 (2006).

662   32.   Reitzer, L. B. T.-R. M. in B. S. Amino Acid Synthesis☆. in (Elsevier, 2014).

663   doi:https://doi.org/10.1016/B978-0-12-801238-3.02427-2

664